

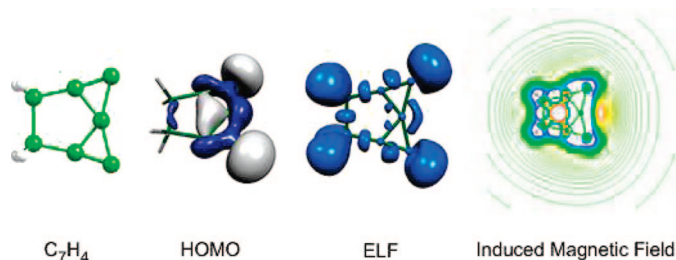
## Planar Tetracoordinate Carbons in Cyclic Semisaturated Hydrocarbons

Nancy Perez-Peralta,<sup>†</sup> Mario Sanchez,<sup>†</sup> Jesus Martin-Polo,<sup>†</sup> Rafael Islas,<sup>†</sup> Alberto Vela,<sup>\*,‡</sup> and Gabriel Merino<sup>\*,†</sup>

Facultad de Química, Universidad de Guanajuato, Noria Alta s/n C.P. 36050, Guanajuato, Gto. México, and Departamento de Química, Centro de Investigación y de Estudios Avanzados, A. P. 14-740, México, D.F. 07000, México

*gmerino@quijote.ugto.mx; avela@cinvestav.mx*

Received April 24, 2008



A series of planar tetracoordinate carbon molecules in cyclic semisaturated hydrocarbons resulting from the combination of the C<sub>5</sub><sup>2-</sup> skeleton with saturated hydrocarbon fragments is reported. The electronic stabilization and the bonding situation are studied through the analyses of molecular orbitals and the electron localization function. The magnetic properties are also revised, giving particular attention to the induced magnetic field. These systems are the first semisaturated cycles containing a planar tetracoordinate carbon stabilized only by electronic factors.

A keystone of organic chemistry is, undoubtedly, the tetrahedral symmetry adopted by the carbon atom when it is tetracoordinated. In an effort to find mechanisms that could challenge this paradigm, in 1970, Hoffmann, Alder, and Wilcox suggested rules to stabilize molecules with a planar tetracoordinate carbon (ptC).<sup>1</sup> Motivated by this interesting idea, several groups have successfully suggested and, in some cases, experimentally characterized molecules containing ptC atoms (for leading reviews see refs 2–9) or even having a higher

coordination.<sup>10–17</sup> It is not pretentious to say that the recent ptC research is opening a new age in carbon chemistry.

Carbon flatland, as Keese has called it,<sup>5</sup> has its own rules: when methane is forced to acquire a planar D<sub>4h</sub> structure, only two of the 2p orbitals can mix with the 2s orbital, leaving a single 2p orbital without the proper symmetry to combine with

<sup>†</sup> Universidad de Guanajuato.

<sup>‡</sup> Centro de Investigación y de Estudios Avanzados.

(1) Hoffmann, R.; Alder, R. W.; Wilcox, C. F. *J. Am. Chem. Soc.* **1970**, *92*, 4992.

(2) Sorger, K.; Schleyer, P. v. R. *THEOCHEM J. Mol. Struct.* **1995**, *338*, 317.

(3) Collins, J. B.; Dill, J. D.; Jemmis, E. D.; Apeloig, Y.; Schleyer, P. v. R.; Seeger, R.; Pople, J. A. *J. Am. Chem. Soc.* **1976**, *98*, 5419.

(4) Rottger, D.; Erker, G. *Angew. Chem., Int. Ed.* **1997**, *36*, 812.

(5) Keese, R. *Chem. Rev.* **2006**, *106*, 4787.

(6) Merino, G.; Mendez-Rojas, M. A.; Vela, A.; Heine, T. *J. Comput. Chem.* **2007**, *28*, 362.

(7) Minyaev, R. M.; Gribanova, T. N.; Minkin, V. I.; Starikov, A. G.; Hoffmann, R. *J. Org. Chem.* **2005**, *70*, 6693.

(8) Minkin, V. I.; Minyaev, R. M.; Hoffmann, R. *Usp. Khim.* **2002**, *71*, 989.

(9) Radom, L.; Rasmussen, D. R. *Pure Appl. Chem.* **1998**, *70*, 1977.

(10) Exner, K.; Schleyer, P. v. R. *Science* **2000**, *290*, 1937.

(11) Wang, Z. X.; Schleyer, P. v. R. *Science* **2001**, *292*, 2465.

(12) Minyaev, R. M.; Gribanova, T. N.; Starikov, A. G.; Minkin, V. I. *Dokl. Chem.* **2002**, *382*, 41.

(13) Li, S. D.; Miao, C. Q.; Guo, J. C.; Ren, G. M. *J. Am. Chem. Soc.* **2004**, *126*, 16227.

(14) Ito, K.; Chen, Z. F.; Corminboeuf, C.; Wannere, C. S.; Zhang, X. H.; Li, Q. S.; Schleyer, P. v. R. *J. Am. Chem. Soc.* **2007**, *129*, 1510.

(15) Wang, L. M.; Huang, W.; Averkiev, B. B.; Boldyrev, A. I.; Wang, L. S. *Angew. Chem., Int. Ed.* **2007**, *46*, 4550.

(16) Islas, R.; Heine, T.; Ito, K.; Schleyer, P. v. R.; Merino, G. *J. Am. Chem. Soc.* **2007**, *129*, 14767.

(17) Pei, Y.; Zeng, X. C. *J. Am. Chem. Soc.* **2008**, *130*, 2580.

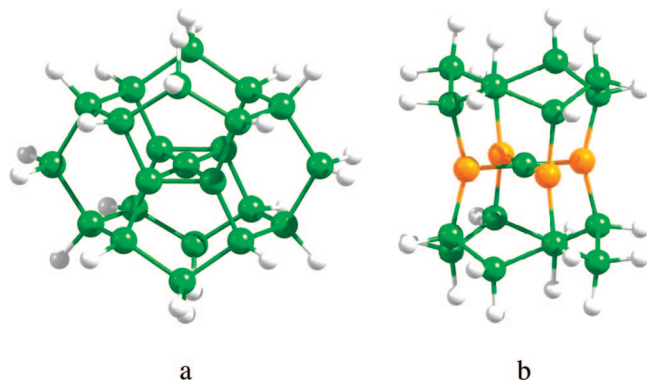


**FIGURE 1.** (a) Rasmussen and Radom's proposal.<sup>18</sup> (b) Wang and Schleyer's proposal.<sup>20</sup> Green and orange spheres correspond to carbon and boron atoms, respectively. White spheres represent hydrogen atoms.

the previous valence orbitals.<sup>1,5</sup> This fact leaves a lone pair perpendicular to the molecular plane that will not contribute to the binding of the molecule. Thus, by lowering the symmetry of methane from  $T_d$  to  $D_{4h}$ , only six electrons occupy three bonding orbitals, contrasting with the four bonding pairs present in  $T_d$  methane. From this analysis, Hoffmann et al. suggested that a strategy to stabilize a ptC is to include the lone pair in the bonding framework by replacing one or more hydrogen atoms with good  $\sigma$ -donor/ $\pi$ -acceptor ligands or, alternatively, by incorporating the lone pair into a  $(4n + 2)\pi$  delocalized system.<sup>1</sup> Another strategy involves some geometrical restrictions, i.e., the central carbon atom and its nearest neighbors will be mechanically forced to be planar by using rings and cages. However, the experimental efforts done so far to isolate one of these mechanically stabilized ptC molecules have been fruitless.<sup>18</sup>

In 1997, Keese stated that "despite considerable computational efforts, no structures with a planar  $C(C)_4$  structure have been found."<sup>19</sup> Two years later, doubly bridged octaplanes were proposed in silico by Rasmussen and Radom (Figure 1a).<sup>18</sup> A similar strategy was used to design charge-compensated octaplanes by Wang and Schleyer (Figure 1b).<sup>20</sup> As one can clearly see in Figure 1, in both cases, a mechanical approach was employed to stabilize the ptC.

Recently, we have analyzed the bonding and stability of new planar tetracoordinate carbon molecules.<sup>21–24</sup> In 2003, some of the authors presented the smallest carbon cluster containing a ptC, namely, the dianion  $C_5^{2-}$ .<sup>21</sup> DFT and high-level ab initio calculations showed that **1** is a minimum on the potential energy surface (PES). The addition of cations resulted in stable compounds (salts) preserving the ptC structure. It was found that the interaction of the parental  $C_5^{2-}$  skeleton with the alkali atoms is essentially ionic, with a remarkable transferability of properties from the isolated dianion to the  $C_5M_2$  salts.<sup>22</sup> The analysis of the molecular orbitals and the magnetic response showed that, indeed, electron delocalization plays a significant

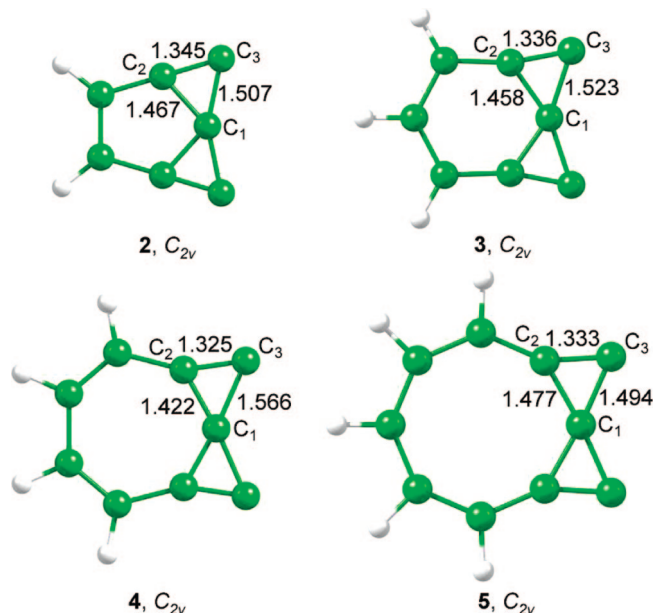
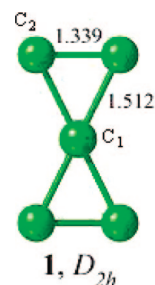


**FIGURE 2.** Optimized structures of cyclic unsaturated hydrocarbons containing a ptC. Geometries were optimized with B3LYP/6-311++G(d,p). Bond lengths are given in angstroms.

role in stabilizing these ptC molecules. With these designing elements at hand, it was possible to find polymers and extended two- and three-dimensional systems containing ptCs within the  $C_5^{2-}$  fragment.<sup>23</sup>



In recent years, we increased the number of examples belonging to the brave new world of  $C_5^{2-}$ .<sup>5</sup> Candidates were obtained by combining the parental  $C_5^{2-}$  dianion with an unsaturated hydrocarbon.<sup>24</sup> These structures are depicted in Figure 2. The harmonic analysis shows that all of them are local minima on their respective PES with a smallest positive vibrational frequency of around  $100\text{ cm}^{-1}$ . In that work it was concluded that the balance between electron delocalization and ring strain determines the stability of these cycles.

In this work a new series of ptC-containing molecules that result from the combination of the  $C_5^{2-}$  skeleton (unsaturated fragment) with saturated hydrocarbon fragments is presented. As it will be shown, the resultant semisaturated cycles are local minimum. The electronic stabilization and the prevailing bonding situation are studied through the analysis of molecular orbitals and the electron localization function (ELF).<sup>25</sup> The magnetic properties are revised, giving particular attention to the induced magnetic field.<sup>26,27</sup> These systems are the first

(18) Rasmussen, D. R.; Radom, L. *Angew. Chem., Int. Ed.* **1999**, *38*, 2876.

(19) Thommen, M.; Keese, R. *Synlett* **1997**, 231.

(20) Wang, Z.-X.; Schleyer, P. v. R. *J. Am. Chem. Soc.* **2001**, *123*, 994.

(21) Merino, G.; Mendez-Rojas, M. A.; Vela, A. *J. Am. Chem. Soc.* **2003**, *125*, 6026.

(22) Merino, G.; Mendez-Rojas, M. A.; Beltran, H. I.; Corminboeuf, C.; Heine, T.; Vela, A. *J. Am. Chem. Soc.* **2004**, *126*, 16160.

(23) Pancharatna, P. D.; Mendez-Rojas, M. A.; Merino, G.; Vela, A.; Hoffmann, R. *J. Am. Chem. Soc.* **2004**, *126*, 15309.

(24) Perez, N.; Heine, T.; Barthel, R.; Seifert, G.; Vela, A.; Mendez-Rojas, M. A.; Merino, G. *Org. Lett.* **2005**, *7*, 1509.

(25) Becke, A. D.; Edgecombe, K. E. *J. Chem. Phys.* **1990**, *92*, 5397.

(26) Merino, G.; Heine, T.; Seifert, G. *Chem. Eur. J.* **2004**, *10*, 4367.

(27) Heine, T.; Islas, R.; Merino, G. *J. Comput. Chem.* **2007**, *28*, 302.

semisaturated cycles containing a planar tetracoordinate carbon atom that are stabilized only by electronic factors.

## Computational Details

Geometry optimizations and electronic structure calculations were performed using Gaussian 98.<sup>28</sup> Structures were optimized using Becke's exchange (B),<sup>29</sup> Lee, Yang, and Parr (LYP) correlation,<sup>30</sup> within the hybrid functional (B3LYP) approach, as implemented in Gaussian 98. All calculations were done using the 6-311++G(d,p) basis set.<sup>31</sup> Every stationary point on the PES was characterized by a harmonic analysis using the same theoretical methodology as that used in the geometry optimization. The zero-point energy correction scaled by 0.9806, as recommended by Scott and Radom,<sup>32</sup> was also calculated. Minima connected by a given transition state were confirmed by intrinsic reaction coordinate (IRC) calculations.<sup>33</sup> IRC calculations were done with the Gonzalez and Schlegel algorithm<sup>34</sup> that has been recently implemented in the program deMon2k.<sup>35</sup> These calculations were done with the PBE exchange-correlation energy functional<sup>36</sup> and DZVP orbital basis set,<sup>37</sup> and an automatically generated Hermite Gaussian auxiliary set GEN-A2<sup>38</sup> that, following Pople's notation, will be denoted by PBE/DZVP/GEN-A2. (The Cartesian coordinates and energies are given in Supporting Information.) To gain further understanding of the chemical bonding in these ptC molecules, the electron localization function was analyzed using the TopMod program.<sup>39</sup>

The induced magnetic field was performed using PW91/IGLO-III.<sup>40,41</sup> The shielding tensors were computed using the IGLO method.<sup>42</sup> The deMon2k program<sup>35</sup> was used to compute the molecular orbitals and the deMon-NMR<sup>43,44</sup> package for the shielding tensors. Induced magnetic fields were computed in ppm of the external fields. Assuming an external magnetic field of  $\mathbf{B}^{\text{ext}} = 1.0$  T, the unit of the induced field is  $1.0 \mu\text{T}$ , which is equivalent to 1.0 ppm of the shielding tensor. For the rendering of the induced magnetic

field, the molecules were oriented in the following way: the external field was applied perpendicular to the  $\text{C}(\text{C})_4$  plane. The induced magnetic field has been applied to understand electron delocalization of classical organic rings,<sup>26</sup> borazine,<sup>45</sup> and aluminum clusters.<sup>46</sup> The programs VU<sup>47</sup> and Molekel<sup>48</sup> were used for the visualization of the molecular fields.

Since deMon2k and deMon-NMR have no possibility to do hybrid calculations, only GGA calculations were done with the latter programs to obtain the IRC paths and the induced magnetic fields. However, it is worth pointing out that the structural parameters obtained with B3LYP and PBE are in very good agreement. The IRC paths and the induced magnetic fields presented in this work are used for qualitative purposes, and as long as they are of good quality, the main conclusions drawn from them will not be affected. The PBE functional was used to obtain the IRCs from a nonempirical GGA and the PW91/IGLO methodology is used following the recommendation done by the authors of the implementation of the magnetic response properties in deMon.<sup>44</sup>

## Results and Discussion

**Structures.** Semisaturated ptC candidates were designed by combining the  $\text{C}_5^{2-}$  moiety with a saturated hydrocarbon fragment. The removal of two hydrides from ethane, propane, butane, and pentane provided the corresponding dications, which interact with  $\text{C}_5^{2-}$  to yield the neutral closed-shell semisaturated five-, six-, seven-, and eight-membered ring systems, respectively. This strategy is similar to that used previously to design unsaturated organic cycles containing the ptC skeleton. The vertical singlet-triplet energy differences,  $\Delta E(\text{S-T}) = E(\text{Triplet}) - E(\text{Singlet})$ , reported in Table 1, show that all singlets are more stable than their corresponding triplets, by approximately 88 kcal mol<sup>-1</sup>. Thus, the discussion below will focus on the closed-shell systems only.

Figure 3 depicts the optimized structures of the title compounds calculated at the B3LYP/6-311++G(d,p) level. The harmonic analysis shows that structures **6a–9a** are local minima on their corresponding PES with lowest vibrational frequencies ( $\nu_{\text{min}}$ ) of around 100 cm<sup>-1</sup> (see Table 1).

From the bond distances shown in Figure 3, one can see that while the  $\text{C}_1\text{—C}_3$  bond lengths are approximately 0.1 Å larger than the  $\text{C}_1\text{—C}_2$  distances, the  $\text{C}_2\text{—C}_3$  distance ( $\sim 1.33$  Å, which is close to a delocalized double bond) is almost unchanged with respect to that found in the free dianion (1.339 Å). Similar to their unsaturated cyclic congeners,<sup>24</sup> the bonds between the ptC atom and the surrounding carbons have a single bond character. This observation is supported further by the values obtained for the Wiberg bond indexes (Table 1), which indicate that the bond order of the ptC atom with its surrounding neighbor atoms is in the range of 0.81–1.10. It is also worth noting that, similarly to the saturated systems studied previously, the  $\text{C}_5$  skeleton is remarkably preserved, where structure **6a** is the one showing the larger distortion from the free dianion.

Interestingly, the NBO charges of the  $\text{C}(\text{C})_4$  skeleton are very similar in all of the neutral systems ( $-0.15$  to  $-0.12$ ) and are four times smaller than in the unsaturated anion compounds (**2** and **4**). This fact is in line with the previous observation about the transferability of properties of the  $\text{C}(\text{C})_4$  skeleton. Dipole

(28) Frisch, M. J.; Trucks, G. W.; Schlegel, H. B.; Scuseri, G. E.; Robb, M. A.; Cheeseman, J. R.; Zakrzewski, V. G.; Montgomery, J.; Stratmann, R. E.; Burant, J. C.; Dapprich, S.; Millam, J. M.; Daniels, A. D.; Kudin, K. N.; Strain, M. C.; Farkas, O.; Tomasi, J.; Barone, V.; Cossi, M.; Cammi, R.; Mennucci, B.; Pomelli, C.; Adamo, C.; Clifford, S.; Ochterski, J.; Petersson, G. A.; Ayala, P. Y.; Cui, Q.; Morokuma, K.; Malick, D. K.; Rabuck, A. D.; Raghavachari, K.; Foresman, J. B.; Cioslowski, J.; Ortiz, J. V.; Baboul, A. G.; Stefanov, B. B.; Liu, G.; Liashenko, A.; Piskorz, P.; Komaromi, I.; Gomperts, R.; Martin, R. L.; Fox, D. J.; Keith, T.; Al-Laham, M. A.; Peng, C. Y.; Nanayakkara, A.; Gonzalez, C.; Challacombe, M.; Gill, P. M. W.; Johnson, B.; Chen, W.; Wong, M. W.; Andres, J. L.; Gonzalez, C.; Head-Gordon, M.; Replogle, E. S.; Pople, J. A. *Gaussian 98; Revision A.7*; Gaussian, Inc.: Pittsburgh, PA, 1998.

(29) Becke, A. D. *J. Chem. Phys.* **1993**, *98*, 5648.

(30) Lee, C. T.; Yang, W. T.; Parr, R. G. *Phys. Rev. B: Condens. Matter* **1988**, *37*, 785.

(31) Krishnan, R.; Binkley, J. S.; Seeger, R.; Pople, J. A. *J. Chem. Phys.* **1980**, *72*, 650.

(32) Scott, A. P.; Radom, L. *J. Phys. Chem.* **1996**, *100*, 16502.

(33) Fukui, K. *Acc. Chem. Res.* **1981**, *14*, 363.

(34) Gonzalez, C.; Schlegel, H. B. *J. Chem. Phys.* **1989**, *90*, 2154.

(35) Köster, A. M.; Calaminici, P.; Casida, M. E.; Flores-Moreno, R.; Gaudtner, G.; Goursot, A.; Heine, T.; Ipatov, A.; Janetzko, F.; del Campo, J. M.; Patchkovskii, S.; Reveles, J. U.; Salahub, D. R.; Vela, A. deMon 2K, Cinvestav, Mexico City, 2006.

(36) Perdew, J. P.; Burke, K.; Ernzerhof, M. *Phys. Rev. Lett.* **1996**, *77*, 3865.

(37) Godbout, N.; Salahub, D. R.; Andzelm, J.; Wimmer, E. *Can. J. Chem.* **1992**, *70*, 560.

(38) Calaminici, P.; Janetzko, F.; Köster, A. M.; Mejia-Olivera, R.; Zuniga-Gutierrez, B. *J. Chem. Phys.* **2007**, *126*, 044108.

(39) Noury, S.; Krokidis, X.; Fuster, F.; Silvi, B. Universite Pierre et Marie Curie: Paris, 1997.

(40) Perdew, J. P.; Wang, Y. *Physical Review B: Condensed Matter* **1992**, *45*, 13244.

(41) Kutzelnigg, W.; Fleischer, U.; Schindler, M. *The IGLO-Method: Ab Initio Calculation and Interpretation of NMR Chemical Shifts and Magnetic Susceptibilities*; Springer-Verlag: Heidelberg, 1990; Vol. 23.

(42) Kutzelnigg, W. *Isr. J. Chem.* **1980**, *19*, 193.

(43) Malkin, V. G.; Malkina, O. L.; Reviakine, R.; Schimmelpfennig, B.; Arbuznikov, V.; Kaupp, M. 2001. We write the Cartesian shielding tensor directly from the subroutine SIGOUT.f in deMon-NMR.

(44) Malkin, V. G.; Malkina, O. L.; Salahub, D. R. *Chem. Phys. Lett.* **1993**, *204*, 80.

(45) Islas, R.; Chamorro, E.; Robles, J.; Heine, T.; Santos, J. C.; Merino, G. *Struct. Chem.* **2007**, *18*, 833.

(46) Islas, R.; Heine, T.; Merino, G. *J. Chem. Theory Comput.* **2007**, *3*, 775.

(47) Ozell, B.; Camarero, R.; Garon, A.; Guibault, F. *Finite Elem. Anal. Des.* **1995**, *19*, 295.

(48) Portmann, S.; Luthi, H. P. *Chimia* **2000**, *54*, 766.

TABLE 1. Calculated Molecular Properties of Cyclic Unsaturated and Saturated Hydrocarbons Containing a ptC (see Figures 2 and 3)

	molecular charge	$\Delta E^a$	$\Delta E_{TS}^b$	$\nu_{\min}^c$	WBI <sup>d</sup> (C <sub>1</sub> –C <sub>2</sub> )	WBI <sup>d</sup> (C <sub>1</sub> –C <sub>3</sub> )	IP <sup>e</sup>	global hardness <sup>f</sup>	$\Delta E(S-T)^g$	$q_{C(C)_4}^h$	$\mu^i$
<b>2</b>	0	–9.5	9.1	246	0.93	0.98	9.8	10.5	53.1	–0.12	5.8
<b>3</b>	–1	–6.7	5.8	167	1.00	0.91	1.9	5.5	35.9	–0.49	6.2
<b>4</b>	0	–12.1	7.0	101	1.10	0.80	8.9	9.2	41.9	–0.15	6.9
<b>5</b>	–1	–26.6	2.4	150	0.90	0.98	3.0	6.5	60.9	–0.46	6.4
<b>6a</b>	0	–7.0	9.0	96	1.05	0.86	9.7	10.4	88.0	–0.12	6.7
<b>7a</b>	0	–6.0	8.2	136	1.05	0.86	9.6	10.3	87.8	–0.14	7.2
<b>8a</b>	0	–19.1	6.5	113	1.10	0.82	9.7	10.5	86.9	–0.14	7.2
<b>9a</b>	0	–30.7	6.3	80	1.10	0.81	9.8	10.6	88.6	–0.15	7.3

<sup>a</sup> Difference in energy between the open structure and the ptC molecule given in kcal mol<sup>–1</sup>. <sup>b</sup> Difference energy between the ptC molecule and the transition state related to the opening process given in kcal mol<sup>–1</sup>. <sup>c</sup> Lowest vibrational frequencies in cm<sup>–1</sup>. <sup>d</sup> Wiberg bond indices. <sup>e</sup> Ionization potentials calculated using the Koopmans' theorem at the HF/6–311++G(d,p) level of theory given in eV. <sup>f</sup> Global hardness is calculated using the HF/6–311++G(d,p) frontier orbital energies within the finite differences approach and using Koopmans theorem given in eV. <sup>g</sup> Vertical singlet-triplet gaps in kcal mol<sup>–1</sup>. See text. <sup>h</sup> Natural charges of the C(C)<sub>4</sub> fragment. <sup>i</sup> Dipole moments are given in debye.

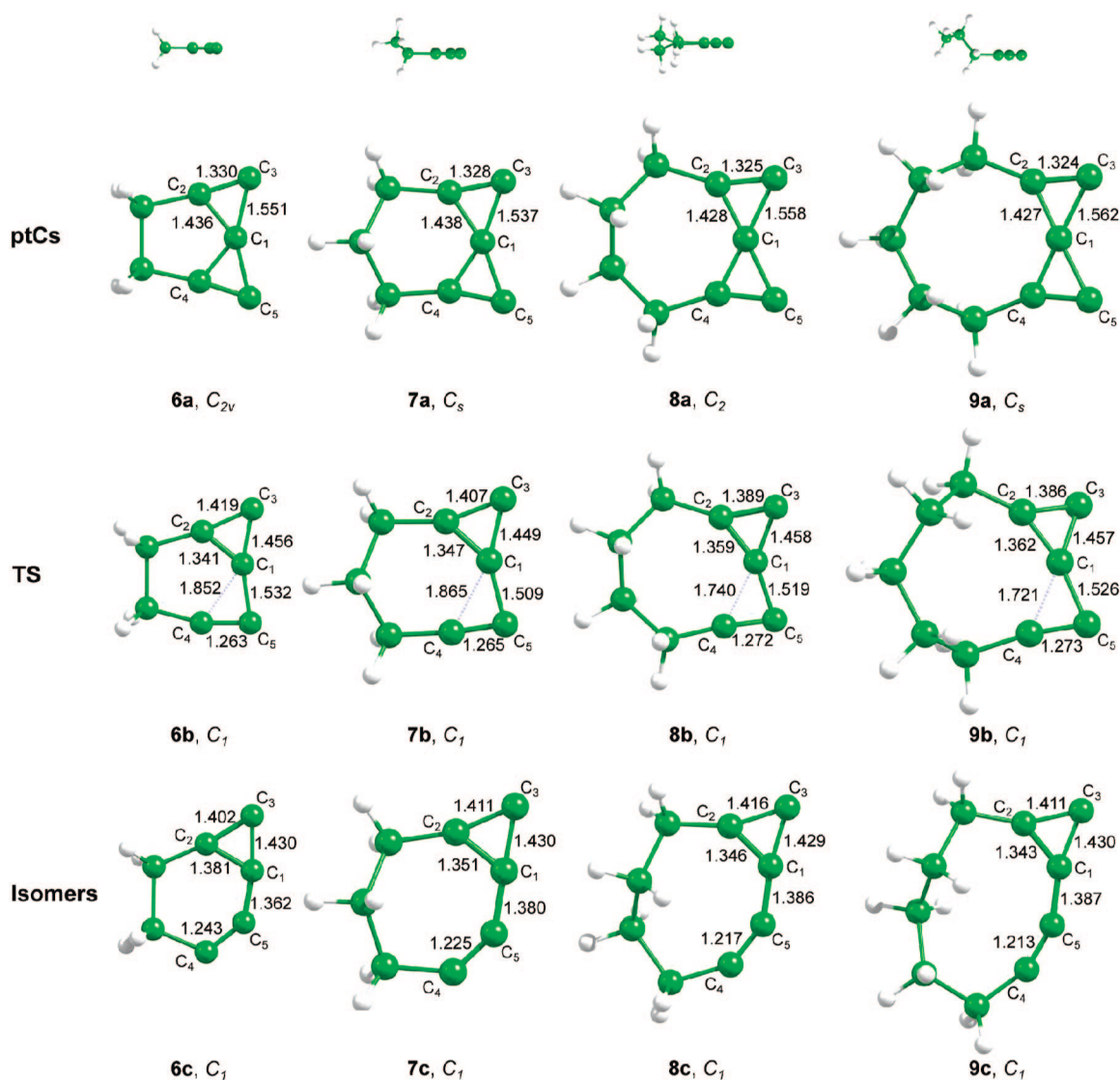


FIGURE 3. Stationary points on the PES of cyclic semisaturated hydrocarbons containing a ptC. From top to bottom, a side and a top view of the ptC containing structure, the transition state (TS) involved in the ring-opening process, and their ring-opening related isomers are depicted. All structures were optimized with B3LYP/6-311++G(d,p). All bond lengths are given in angstroms.

moments were also calculated. The dipole moment values are substantial, lying in the range of 6.7–7.3 D, and suggest that these neutral hydrocarbons can accommodate an extra electron

according to the dipole-bound anion model.<sup>49,50</sup> Note that the

(49) Gutowski, M.; Skurski, P.; Jordan, K. D.; Simons, J. *Int. J. Quantum Chem.* **1997**, *64*, 183.

(50) Jordan, K. D.; Wang, F. *Annu. Rev. Phys. Chem.* **2003**, *54*, 367.

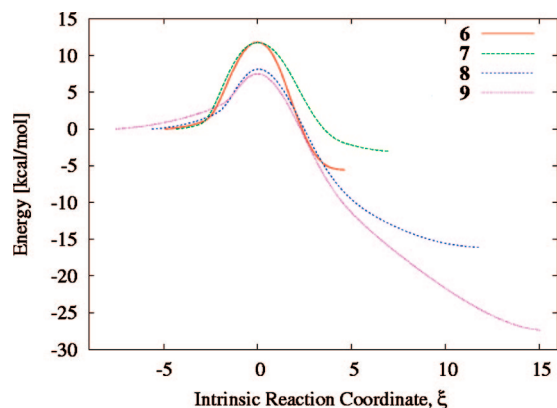


**FIGURE 4.** Reaction paths for the ring-opening process of the title compounds calculated by the IRC method with the PBE/DZVP/GEN-A2 methodology without ZPE correction.

variation of the dipole moment in this series of molecules provides a measure of the relative abilities of the saturated fragment to attract electrons.

**Ring-Opening Process.** Even though these structures are local minima, their experimental detection strongly depends on the magnitudes of the energy barriers that prevent them from isomerization or fragmentation. The probable transition states are shown in Figure 3. To determine if both minima are connected by these transition states, an intrinsic reaction path (IRC) was traced. As depicted in Figure 4, the IRCs smoothly lead to both minima, confirming that structures **6b–9b** are in fact the true transition states related to the ring-opening processes.

As expected, the ring-opening processes are accompanied by small activation barriers, lying in the range of 6–9 kcal mol<sup>-1</sup>, including the scaled zero point energy correction (Table 1). These transition barriers are three times higher than those reported by the groups of Esteves<sup>51</sup> and Sastry<sup>52–54</sup> for neutral hydrocarbons containing a ptC. Interestingly, the ring-opening barriers are similar to those obtained for the neutral unsaturated ptC systems (**2** vs **6a** and **4** vs **8a**; Table 1).

Geometrical changes induced by the ring opening are apparent (Figure 3). At the transition state, the C<sub>2</sub>–C<sub>3</sub> bond distance is lengthened by 0.06–0.08 Å, acquiring a single bond character. In contrast, the C<sub>4</sub>–C<sub>5</sub> bond length is reduced from 1.33 to 1.26 Å, indicating the probable formation of a triple bond. All distances around C<sub>1</sub> are reduced, except of course that related to the ring opening. At the TS, the C<sub>1</sub>–C<sub>4</sub> bond distance is 1.852 Å for structure **6b**, and 1.721 Å for **9b**. Clearly, these ring-opening processes have an early TS, and consequently, the structural relaxation to go from the TS to the isomer is large (compare structures **b** with **c** in Figure 3).

The ring-opening barrier values are interesting. Raising the angular tension on the smaller rings when going from ptC molecule to the “open” form contributes to increase the reaction barrier energy. Thus, smaller rings (e.g., **6** and **7**) have higher barriers than larger rings (e.g., **8** and **9**). The release of tension on the larger rings is also noticeable. Both, the transition states and the final products are benefited by increasing the ring size

since the triple bond in these structures is less stressed (more linear) than in the smaller rings.

**Electronic Structure.** Figure 5 shows the highest occupied molecular orbitals (HOMOs) and the occupied molecular orbitals (MOs) with the largest contribution from the 2p orbitals perpendicular to the C<sub>5</sub> plane that will be called π-MOs. From Figure 5, the multicentric character prevailing in the bonding of these structures is evident. Note that the π-1 MO is distributed over the C(C)<sub>4</sub> skeleton, and its shape within each ring (Figure 5) resembles that of the occupied π-orbital of an aromatic cyclopropenium cation. The p orbital perpendicular to the C(C)<sub>4</sub> plane is involved in the formation of latter π-MO and together with π-2 MO contribute to the double-bond character of the C<sub>2</sub>–C<sub>3</sub> bond. Again, this p-orbital delocalization, or multicenter participation, is one of the fundamental electronic mechanisms that stabilize the ptC structures presented herein.

It should be kept in mind that stabilization of the title systems cannot be fully explained by the incorporation of the C<sub>5</sub><sup>2-</sup> skeleton as part of a delocalized ring as in molecules **2–5**. Let us compare the neutral analogue systems **2** versus **6a**. While the total number of π electrons in **2** is six, this number is only four for **6a**. Ironically, **2** is thermodynamically less stable than **6a** with respect to their open ring structures. However, their ring-opening barriers are similar. Now, the comparison of **4** with **8a**, which have eight and four π electrons, respectively, shows the opposite trend. Thus, it is possible to conclude that the total π electron count seems to play a role in the thermodynamic stability but not in the ring-opening kinetics of these ptC hydrocarbons.

Further support about stability of the semisaturated hydrocarbons reported here is provided by the analysis of the energies involved in one-electron removal processes, i.e., in the ionization potential (IP). For example, using Koopmans’s theorem, the doubly bridged octaplane proposed by Rasmussen and Radom<sup>18</sup> calculated with HF/6-311++G(d,p) has an IP of 5.2 eV, which is almost as small as that of the lithium atom (5.4 eV).<sup>55</sup> However, according to our calculations, the IPs of **6a–9a** at the HF/6-311++G(d,p) (9.6–9.8 eV; Table 1) resemble those of benzene (9.24 eV<sup>56</sup>). Table 1 also documents their HOMO–LUMO gaps, which are the unrelaxed approximation (Koopmans’s theorem) to the global hardness or, in other words, the difference between the ionization potential and electron affinity. The hardness of the saturated cycles is also as high as benzene (10.3 eV, at the same level of theory), which allows one to conclude that the ptC containing structures proposed herein are stable. It is worth to note that the negative electron affinities predicted by Koopmans theorem are not in agreement with the expected stability of the anion of these ptC-containing hydrocarbons that follows from the dipole-bound anion model. Since the eventual experimental observation of these structures can be done by electron capture techniques, this issue demands a closer analysis that is currently being done in our laboratories with electron propagator methods.

To complement the understanding about the electronic scenario in these compounds, a topological analysis of the ELF<sup>25</sup> was done. The ELF analysis provides a partition of the molecular space in basins, which is consistent with Lewis theory of bonding.<sup>57</sup> Quantitative information is further extracted by

(51) Esteves, P. M.; Ferreira, N. B. P.; Corroa, R. J. *J. Am. Chem. Soc.* **2005**, *127*, 8680.

(52) Priyakumar, U. D.; Sastry, G. N. *Tetrahedron Lett.* **2004**, *45*, 1515.

(53) Priyakumar, U. D.; Reddy, A. S.; Sastry, G. N. *Tetrahedron Lett.* **2004**, *45*, 2495.

(54) Sateesh, B.; Reddy, A. S.; Sastry, G. N. *J. Comput. Chem.* **2007**, *28*, 335.

(55) <http://physics.nist.gov/PhysRefData/IonEnergy/tblNew.html>.

(56) Nemeth, G. I.; Selzle, H. L.; Schlag, E. W. *Chem. Phys. Lett.* **1993**, *215*, 151.

(57) Silvi, B.; Savin, A. *Nature* **1994**, *371*, 683.

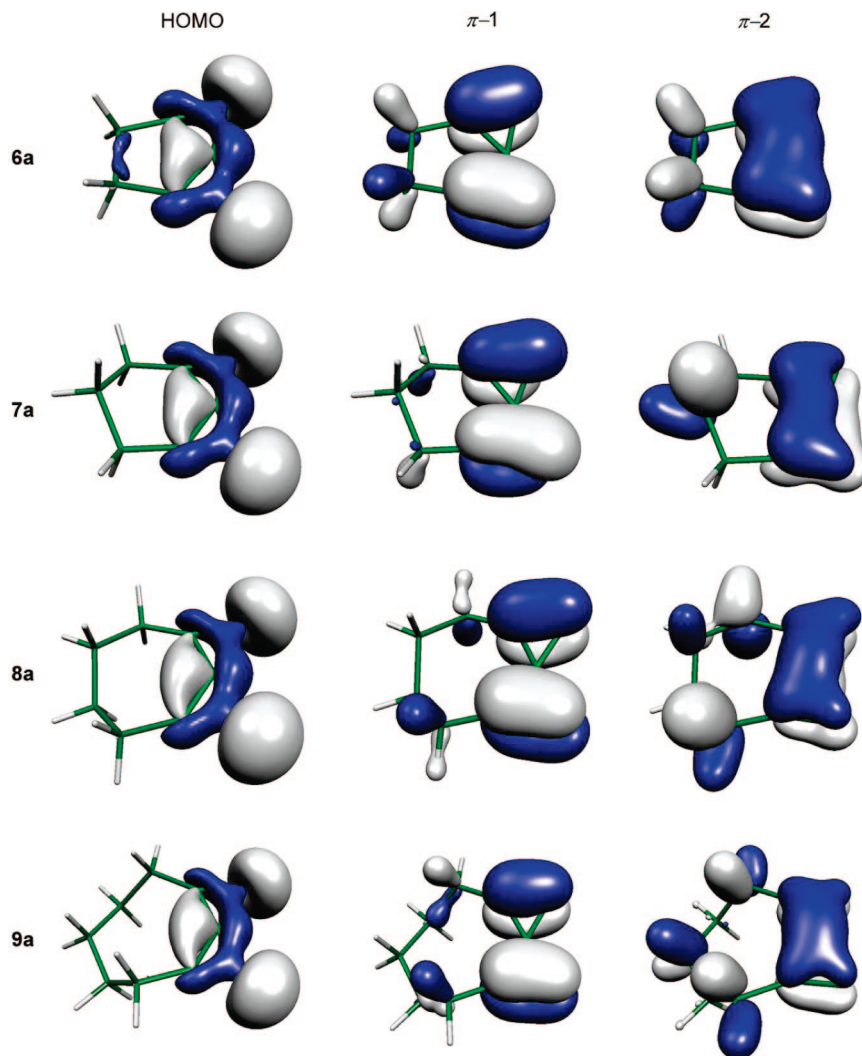


FIGURE 5. HOMO and  $\pi$ -MOs of **6a–9a**.

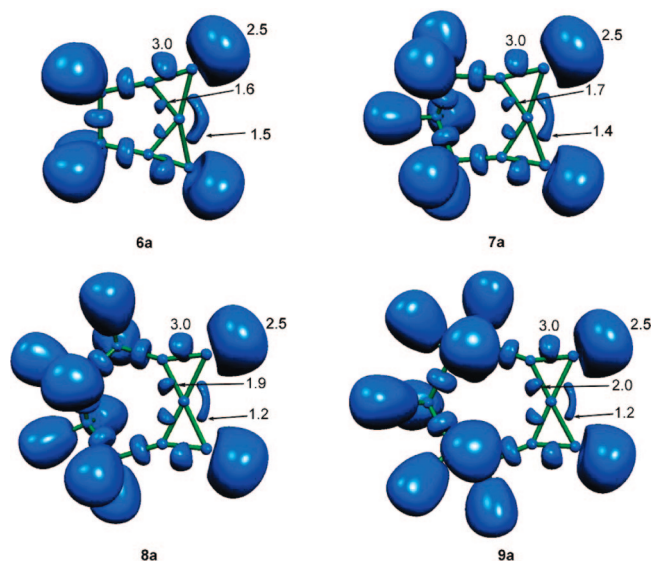
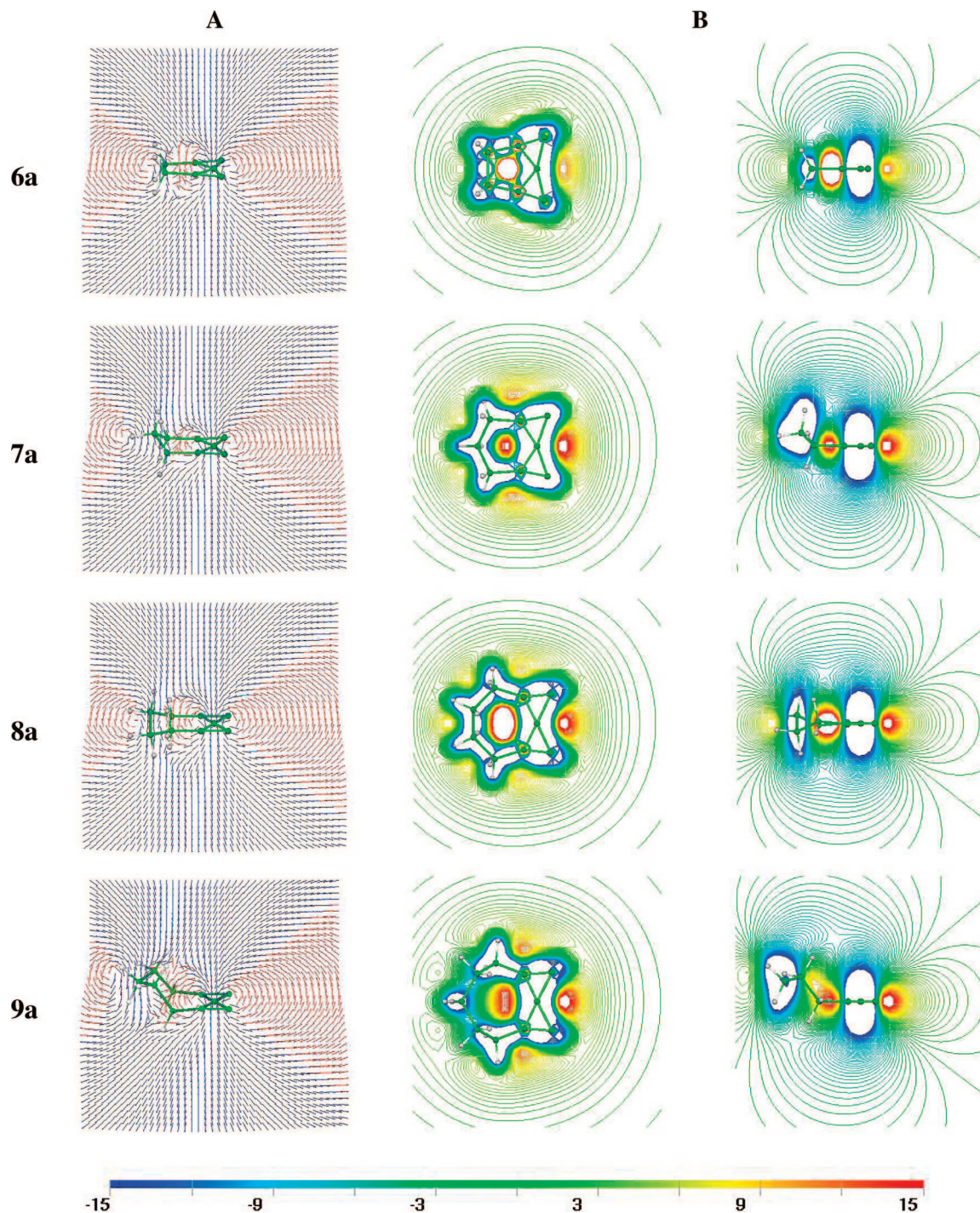


FIGURE 6. ELF isosurfaces (ELF = 0.8) for structures **6a–9a**. The numbers indicate the integration of the electron density in the corresponding basin.

integrating the electron density over these basins. In molecules **6a–9a** there are four basins around the ptC atom, whose populations vary from 1.2 to 2.0  $e^-$  (Figure 6). Interestingly,

as the ring size increases, the  $C_1-C_2$  population basin increases, whereas the  $C_1-C_3$  population basin decreases. The  $C_2-C_3$  population of 3.0  $e^-$  is the same regardless of the size of the



**FIGURE 7.** (A) Induced magnetic field of **6a–9a**. Blue and red areas denote diatropic (shielding) and paratropic (deshielding) regions, respectively. (B) The z-component of  $\mathbf{B}^{\text{ind}}$ , shielding (diatropic, in blue) or enforcing (paratropic, in red) the external field shown in the  $\text{C}(\text{C})_4$  plane and perpendicular to it. The scale is given in ppm.

saturated hydrocarbon bonded to the  $\text{C}(\text{C}_4)$  skeleton. This fact allows one to conclude that this delocalized multicenter bonding provides stability to these structures. This is similar to the electronic mechanism that stabilizes  $\text{C}_5^{2-}$ ,  $\text{CAI}_4^{2-}$ , and  $\text{CB}_6^{2-}$ ,<sup>22</sup> namely, the lone pair of the  $\text{ptC}$  perpendicular to the molecular plane is delocalized over the two triangles of the  $\text{C}(\text{C}_4)$  skeleton. A final noticeable feature in the ELF is the two valence basins that protrude from two of the  $\text{C}(\text{C}_4)$  vertices. These basins have a constant population of  $2.5 e^-$  and they can be attributed to the in-plane lone pairs of these carbon atoms.

**Magnetic Properties.** To detect the presence of probable cyclic electron delocalization, the induced magnetic field was calculated. Figure 7 summarizes the results of the induced magnetic field analysis. In this case, the external field is applied perpendicular to the  $\text{C}(\text{C})_4$  plane directly on the  $\text{ptC}$  atom. Similar to  $\text{C}_5^{2-}$ , all  $\text{ptC}$  molecules studied here have a strong diatropic contributions located inside the three-membered rings. Around the  $\sigma$ -framework of  $\text{C}(\text{C})_4$  skeleton, there is a nodal ring, which separates the shielding from the deshielding region.

Figure 7 also depicts the contour lines and the isolines of the z-component of the induced magnetic field giving a quantification of the magnetic response. The isolines of the z-component of  $\mathbf{B}^{\text{ind}}$  show that the shielding regions (shown in blue) are located around the molecule, while deshielding regions are further outside of the ptC region and include part of the saturated ring (given in red). Furthermore, Figure 7 shows that the response of the molecule to the magnetic field is long-ranged (see above and below the three-membered rings). Therefore, the previous analysis of the induced magnetic field strengthens the conclusion that electron delocalization within the  $\text{C}_5^{2-}$  skeleton enhances the stability of planar tetracoordinate carbons in cyclic semisaturated hydrocarbons.

## Conclusions

In this work a new family of hydrocarbons containing a planar tetracoordinate carbon resulting from the combination of the  $\text{C}_5^{2-}$  moiety with a saturated hydrocarbon fragment is reported. The analyses of the molecular orbitals, electron localization function, and induced magnetic field show that the stability of

these compounds can be attributed to the multicentric nature of the bonding within the  $\text{C}_5^{2-}$  skeleton and its concomitant electron delocalization. This new family of stable ptC containing molecules encourage us to expect that in the near future some of these in silico designed structures will be experimentally detected.

**Acknowledgment.** G.M. gratefully acknowledges support from Conacyt (Grant 57892). A.V. thanks Conacyt for grants 47175-F and CIAM project 2005-C02-51840. N.P.P., R.I., and M.S. thank Conacyt for Ph.D. and postdoctoral fellowships. We thank Jorge Martin del Campo, Keigo Ito, and Miguel Angel Mendez-Rojas for cheerful discussion. We thank the reviewers for their highly valuable comments.

**Supporting Information Available:** Optimized structures of all systems discussed here, including the absolute energy and the zero point energy. This material is available free of charge via the Internet at <http://pubs.acs.org>.

JO800885X